Corrosion Science 80 (2014) 453–460

Contents lists available at ScienceDirect

Corrosion Science

journal homepage: www.elsevier.com/locate/corsci

Long-term high temperature oxidation of CrAl(Y)N coatings in steam atmosphere

S. Mato [a,*], G. Alcalá [a], M. Brizuela [b], R. Escobar Galindo [c], F.J. Pérez [a], J.C. Sánchez-López [d]

[a] Grupo de Investigación de Ingeniería de Superficies y Materiales Nanoestructurados N°910627, Universidad Complutense de Madrid, Facultad de Ciencias Químicas, E-28040 Madrid, Spain
[b] TECNALIA, Parque Tecnológico de San Sebastián, Mikeletegi Pasealekua 2, E-20009 Donostia-San Sebastián, Gipuzkoa, Spain
[c] Instituto de Ciencia de Materiales de Madrid, Consejo Superior de Investigaciones Científicas, E-28049 Madrid, Spain
[d] Instituto de Ciencia de Materiales de Sevilla (CSIC-US), Avda. Américo Vespucio 49, E-41092 Sevilla, Spain

ARTICLE INFO

Article history:
Received 22 July 2013
Accepted 30 November 2013
Available online 12 December 2013

Keywords:
A. Sputtered films
A. Steel
B. EPMA
B. Weight loss
C. High temperature corrosion
C. Oxidation

ABSTRACT

The oxidation resistance of CrAl(Y)N coatings deposited by reactive magnetron sputtering on P92 steel substrates was tested at 650 °C in 100% steam atmosphere up to 2000 h of oxidation. Mass gain measurements and characterisation of coatings and scales after oxidation show the enhanced oxidation resistance provided by the coatings with respect to that of the substrate. The dominant influence of the film microstructure developed due to the presence of an adhesion interlayer of CrN at the coating/substrate interface over Y additions is evidenced. The best performance is achieved by a CrAlN dense coating of around 6 μm without adhesion interlayer.

1. Introduction

Many high temperature applications of hard coatings in industrial processes require additional properties to those related to wear and hardness, like a good oxidation resistance. This is the case of coated tools for casting, machining and forming, as well as power plant components.

Chromium nitride and ternary chromium nitride coatings have become commonly used in the protective ceramic coatings field. Following this approach, important improvements to the mechanical and tribological performance of the initial binary chromium nitride coatings have been achieved by the addition of Al using different deposition techniques [1–4].

Extensive assessments of the corrosion resistance on chromium nitride coatings have been carried out mainly in air. Banakh et al. found an improvement of the corrosion resistance in $Cr_{1-x}Al_xN$ coatings with $0.2 \leqslant x \leqslant 0.63$ compared to pure CrN [5]. They, as well as other authors, associated this improvement with the development of a mixed Cr/Al-rich oxide layer which blocks inward oxygen diffusion preventing further film oxidation [6,7]. Additionally, the introduction of small concentrations of reactive elements such as Y in CrAlN coatings has been shown to increase oxidation resistance and thermal stability [8–10].

Nevertheless, it is known that for some applications the development of coatings with a long-term performance in water vapour media is of special interest. Lifetime of turbine blades, steam pipes and superheater tubes are dramatically compromised by such severe working conditions. The performance of high temperature materials operating in an environment with variable presence of water vapour can differ from that in air. This is the case of steels, whose good response to high temperature oxidation relies on the development of a protective chromium oxide on the surface. The presence of a steam atmosphere changes the oxidation mechanism and oxidation rates, preventing the formation of protective chromia and resulting in a more active corrosion [11]. Also in nitride ceramics it has been shown that the surface oxide layer and the corrosion reaction products developed during oxidation depend on the environment [12].

Therefore, the aim of this work is to contribute to the very limited knowledge on the long-term behaviour of reactive magnetron sputtered CrAl(Y)N coatings deposited on steel, with and without adhesion interlayer, oxidised at high temperature in 100% steam atmosphere. The effect of yttrium doping, film microstructure and coating thickness will also be explored.

2. Experimental procedure

2.1. Materials: substrate and coatings

The substrate material used in this study was P92, a ferritic steel generally used in the manufacture of boiler superheaters,

* Corresponding author.
E-mail address: msmatodi@quim.ucm.es (S. Mato).

0010-938X/$ - see front matter © 2013 Elsevier Ltd. All rights reserved.
http://dx.doi.org/10.1016/j.corsci.2013.11.066

advanced power plant components and steam piping. Its precise composition is shown in Table 1. Specimens of 10 × 10 × 3 mm of size were cut from a sheet, ground up to 600# SiC grit paper and subsequently, the surfaces were thoroughly cleaned in an ultrasonic bath with ethanol.

CrAlN and CrAlYN coatings were deposited on P92 steel specimens using a commercial direct current (d.c.) magnetron sputtering equipment (CemeCon® CC800/8) with four separated rectangular targets of 200 × 88 × 5 mm dimensions. Two targets were 99.9 wt.% Cr, one 99.5 wt.% Al and the last one was 99.5 wt.% Y. Previously, the chamber was evacuated to 1×10^{-4} Pa and the substrate surfaces were sputter-etched with Ar^+ for additional surface cleaning. The deposition process was carried out in a reactive atmosphere of Ar/N_2, applying a d.c. voltage of 110–120 V and with a measured temperature due to plasma effect in the range of 200–400 °C.

Samples were held in the deposition chamber by a welded bar in such a way that allowed three directional deposition to cover all the faces of the substrates. In order to obtain the desired composition in the coatings the sputtering powers were set at 3000 W for the Cr and Al targets while 500 or 1500 W were used for the Y target, maintaining the Ar/N_2 ratio at 1.5.

Four different CrAlN based coatings were deposited for this study: two CrAlN coatings (CrAlN-1 and CrAlN-2) and two CrAlYN coatings (CrAlYN-1 and CrAlYN-2) with varying concentrations of Y (1.7 and 0.4 at.%, respectively).

A layer of CrN of approximately 4 μm of thickness was deposited at the coating/substrate interface to favour the adherence of the coatings. To study the effect of this layer on the coating performance during steam oxidation, the CrN interlayer was absent in one of the CrAlN coatings (CrAlN-1).

Extensive microstructural, mechanical and chemical characterisation of similar coatings with lower thicknesses deposited on Si wafers can be found in a previous publication [13]. There, detailed compositions of those coatings were determined by electron probe microanalysis (EPMA) with a JEOL Superprobe JXA-8200M. The values obtained are presented in Table 2.

2.2. Oxidation tests

P92 substrates and coated samples were oxidised at 650 °C in 100% steam atmosphere up to 2000 h. Conditions for oxidation were chosen to simulate the operation parameters of supercritical turbine engines employed to increase energy efficiency conversion in power plants. Although this approach does not take into account the operating pressure, it provides well-controlled conditions to study the processes involved in oxidation.

The oxidation was carried out in a tubular horizontal furnace at 650 °C connected to a second furnace in which the steam was generated from de-oxygenated water. A detailed description of the experimental set up is shown elsewhere [14].

The oxidation kinetics was determined by mass gain measurements in a five decimal balance. The samples were removed from the furnace at fixed intervals; in the first hours every 24 h and later every 150 h approximately. After each of those intervals the furnace was turned off from the mains. To prevent further oxidation of the samples while the furnace cooled down to room temperature nitrogen was injected into it. The samples were then allowed to dry in a nitrogen atmosphere for eight hours, withdrawn from the furnace, weighed and returned to it for subsequent oxidation. Three specimens of each coating were oxidised to confirm the reproducibility of the data.

Table 1
Composition of the ferritic steel P92 used as substrate (% in weight).

	Cr	V	Ni	Mo	Mn	Si	W	C	Fe
ASTM P92	9.07	0.2	0.06	0.46	0.47	0.02	1.78	0.1	87.84

Table 2
Composition of the deposited coatings by EPMA (at.%).

	Cr	Al	Y	N
CrAlN-1	36.5	8.3	–	55.2
CrAlN-2	39.5	4.6	–	55.9
CrAlYN-1	38.6	5.1	1.7	54.6
CrAlYN-2	39.5	5.2	0.4	54.9

2.3. Characterisation techniques

In order to study the morphology and thicknesses of as-deposited coatings, cross sections of the samples were observed by scanning electron microscopy (SEM) in a JEOL JSM-6400 at 20 kV with a working distance of 15 mm. Furthermore, their chemical compositions were determined by Rutherford backscattering spectroscopy (RBS). RBS experiments were carried out using the 5MV HVEE Tandetron accelerator sited at the Centro de Micro-Análisis de Materiales of Universidad Autónoma de Madrid using 3.700 MeV He^+ ions. The data were interpreted using the RBX program [15].

After oxidation, characterisation of modified coatings and scales was performed on the specimens at different oxidation exposure times. Morphology and thicknesses were studied in planar and cross-section views of the samples after 2000 h of oxidation by SEM. Metallographic preparation for a cross-section examination involved the successive deposition on the surface of a thin gold layer and a thicker layer of electroless nickel, the assembly of selected samples in conductive resin, grinding and polishing down to 1 μm diamond paste. Chemical composition information of scales was achieved by EPMA with a JEOL Superprobe JXA-8900M at 20 kV and 50 nA using a beam diameter of 1.2 μm.

Depth profile analysis of coating elements after 700 h of oxidation were determined by means of glow discharge optical emission spectroscopy (GDOES) employing a Horiba Jobin Yvon RF GD instrument. This equipment was operated in argon plasma of 650 Pa and forward power of 40 W, with a 4 mm diameter copper anode. The wavelengths of the spectral lines used were 130.21 nm for oxygen, 149.26 nm for nitrogen, 371.99 nm for iron, 396.15 nm for aluminium, 425.23 nm for chromium and 371.03 nm for yttrium.

3. Results

3.1. As-deposited coating characterisation

Fig. 1 shows four representative SEM micrographs of the cross sections of the as-deposited coatings. Film thicknesses were measured from these cross-section views and are compiled in Table 3. The comparison of Fig. 1(a), corresponding to the CrAlN-1 coating, with the micrographs obtained for the other coatings (Fig. 1(b)–(d)) evidences the different morphology of the coatings due to the presence, in the latter, of the CrN layer. All the studied coatings have parallel and continuous interfaces. However, in the micrographs of the CrAlN-2, CrAlYN-1 and CrAlYN-2 coatings, the adhesion interlayer at the coating/steel interface shows a rough appearance after polishing, with numerous needle-like features perpendicular to the interfaces. In contrast, the coatings deposited on the CrN adhesion interlayer and the CrAlN-1 coating appear smooth and with low porosity.

Chemical compositions of the as-deposited coatings were determined by RBS. Experimental and simulated spectra displayed in

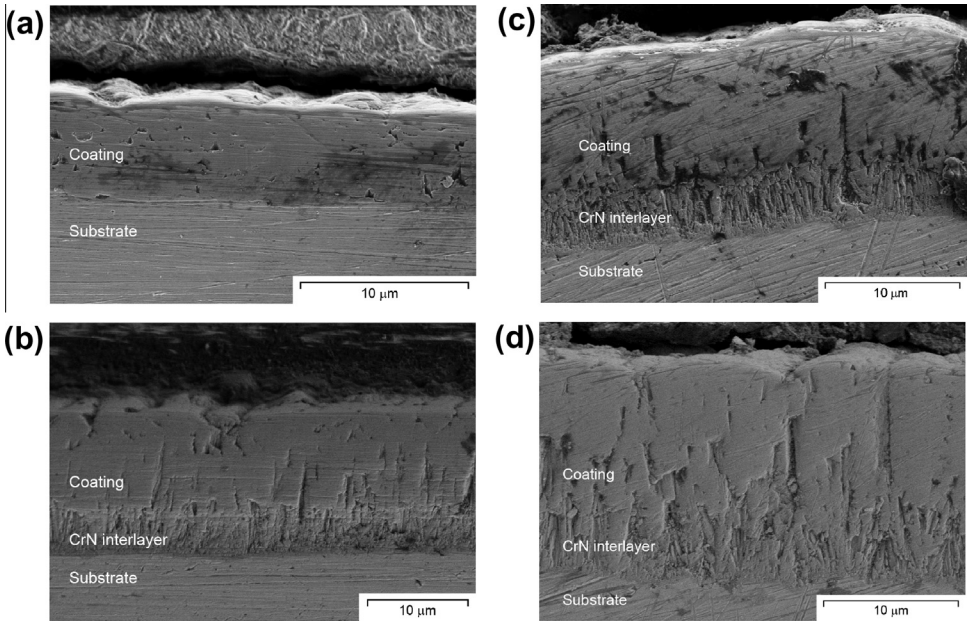

Fig. 1. Scanning electron microscopy of the cross sections of as deposited samples of (a) CrAlN-1, (b) CrAlN-2, (c) CrAlYN-1, and (d) CrAlYN-2 coatings.

Table 3
Composition of the deposited coatings by RBS (at.%) and their thicknesses (in μm) measured from the cross-section SEM micrographs.

	Cr	Al	N	Y	Thickness
CrAlN-1	35–38	7–8	52–57	–	5.9
CrAlN-2	35–40	7–8	50–56	0	15.6
CrAlYN-1	37	9	52	2	14.3
CrAlYN-2	38	7	55	0.5	16.4

Fig. 2 reveal a homogeneous composition throughout the coatings. The slight sequential variations observed are due to the rotation speed of the plate in the deposition chamber. The results summarized in Table 3 are in agreement with those obtained by EPMA for the replica coatings deposited on Si wafers.

3.2. Oxidation kinetics

Fig. 3 displays the mass gain per unit area versus time curves of the substrate and the four coatings. The mass gain represented data are the average of the mass gain per unit area of the three identical specimens oxidised per each coating. The errors of the data correspond to the standard deviation of the measurement at each oxidation time, which are larger than the errors calculated from the instrumental accuracy.

For comparison, the oxidation data obtained for the P92 substrate and those of the studied coatings are presented together. Oxidation of P92 substrate occurs with a large increase in weight due to the formation of a thick scale of iron and chromium oxides [14]. However, the mass gain for the CrAlN-2 and the CrAlYN-based coatings increases rapidly with time in the very first stage of the process stabilizing afterwards at two orders of magnitude smaller than the value measured for the steel, which indicates a lower oxidation rate (inset of Fig. 3). Interestingly, the stabilization of the CrAlYN-based coatings mass gain takes place in the first 72 h of treatment, much faster than in the case of the CrAlN-2 coating which stabilizes after approximately 500 h of oxidation. The oxidation kinetics follows the expected parabolic law up to 1000 h. After this exposure time a mass decrease is identified for the coatings with the CrN adhesion interlayer, being more pronounced for the

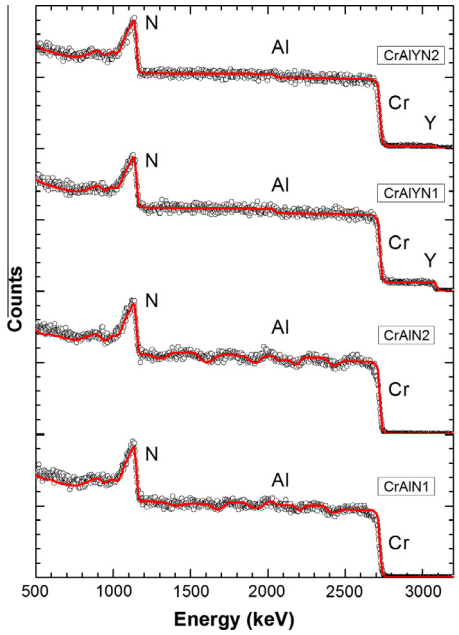

Fig. 2. Experimental and simulated spectra by RBS of as deposited (a) CrAlN-1, (b) CrAlN-2, (c) CrAlYN-1, and (d) CrAlYN-2 coatings.

coatings with yttrium content. In the case of the CrAlN-1 coating without Y-doping and CrN adhesion interlayer, the mass variation with time results in negligible or slightly negative values.

3.3. SEM observations of the oxidised specimens

In Fig. 4 representative micrographs of the surfaces of the coatings after 2000 h of oxidation in 100% steam are disclosed. In all of them, it is possible to distinguish the lines due to the rough surface finishing of the substrate and fine droplets up to 10 μm of diameter approximately (Fig. 4(a)–(d)). The droplets, which are characteristic of the deposition method [3], show identical composition to that of the coating. However, some differences are noticed in this

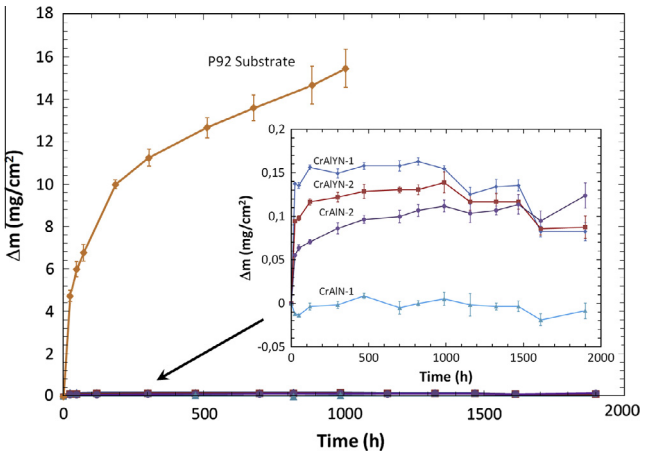

Fig. 3. Mass change per unit area versus time of the substrate P92 up to 1000 h and the nitride coatings under study up to 2000 h at 650 °C in 100% steam atmosphere. The mass change represented in the graph is total mass change calculated by subtracting the mass measured per unit area after each oxidation interval from the initial mass per unit area of the as-received specimen. Mass gain due to the adsorption of oxygen and mass loss due to the de-nitridation process are reflected in the weight variations. The inset shows an enlargement of the part of the graph corresponding to the coated samples.

singular morphology. The surface of the coatings becomes more granular and rougher in the yttrium doped samples. The presence of fine oxidation products of bright appearance decorates the surface of the oxidised coating, particularly the CrAlYN-1 and CrAlN-2 specimens. Finally, the CrAlN-1 sample displays a regular surface with compacted lines and a few isolated white spots.

Fig. 5(a)–(d) shows the backscattered electron images taken for the cross-section views of CrAlN-1, CrAlN-2, CrAlYN-1 and CrAlYN-2 coatings respectively after 2000 h of oxidation. Back-scattered electron mode was employed to enhance contrast between layers with different compositions. Comparing the above pictures with those taken for the initial coatings (Fig. 1), no clear evidence of surface oxidation and film degradation is observed. In contrast to the coatings with the adhesion layer that conserved the two-layered morphology after oxidation, the CrAlN-1 coating discloses a homogeneous appearance with no features.

3.4. Compositional analysis of the as-deposited and oxidised specimens

In order to determine the composition of the modified coatings after 2000 h of oxidation at 650 °C in 100% steam, depth profiles by EPMA are shown in Fig. 6. A protecting nickel layer was deposited prior to sample preparation to avoid delamination of the oxide scale. For the CrAlN-1 coating (Fig. 6(a)) the steady value of nitrogen, aluminium and chromium signals indicates a homogeneous composition through the coating thickness. In the case of the coatings with adhesion interlayer the most significant feature, taking into account the chromium and nitrogen signals, is the oxidation of the chromium nitride layer at the coating/substrate interface (Fig. 6(b)–(d)). Certain oxygen enrichment is detected in the film surfaces as a result of the steam treatment but it is overlapped with that of nickel protecting layer making its evaluation difficult. With the aim of further studying the coating oxidation (inner and outer layer) and ion diffusion processes during the steam tests, analysis by GDOES of samples after 700 h of treatment were carried out in the two CrAlN coatings and in the CrAlYN coating with the highest Y content.

Fig. 7 shows the GDOES profiles for the CrAlN-1, CrAlN-2 and CrAlYN-1 coatings ((a)–(c)). The general behaviour observed is the formation of a surface oxide layer mainly constituted by Al and Cr as a consequence of the exposure to the steam flow at 650 °C. Moreover, in the samples of CrAlN-2 and CrAlYN-1 the formation of the chromium oxynitride in the interlayer with the substrate, detected after 2000 h of oxidation by EPMA, has already started at 700 h. Oxygen contents along the film thickness of the coatings with CrN adhesion interlayer are found in the range 3–8 at.% suggesting its migration through the film inhomogeneities and columnar boundaries (particularly in the yttrium-doped sample). Regarding the iron signal, some Fe diffusion at the interface with the coating cannot be ruled out. However, the authors tend to ascribe such iron profile to mixing effects due to a non-flat geometry of the crater created during GDOES analysis (see for example [16]). This effect is enhanced by a roughening of the crater

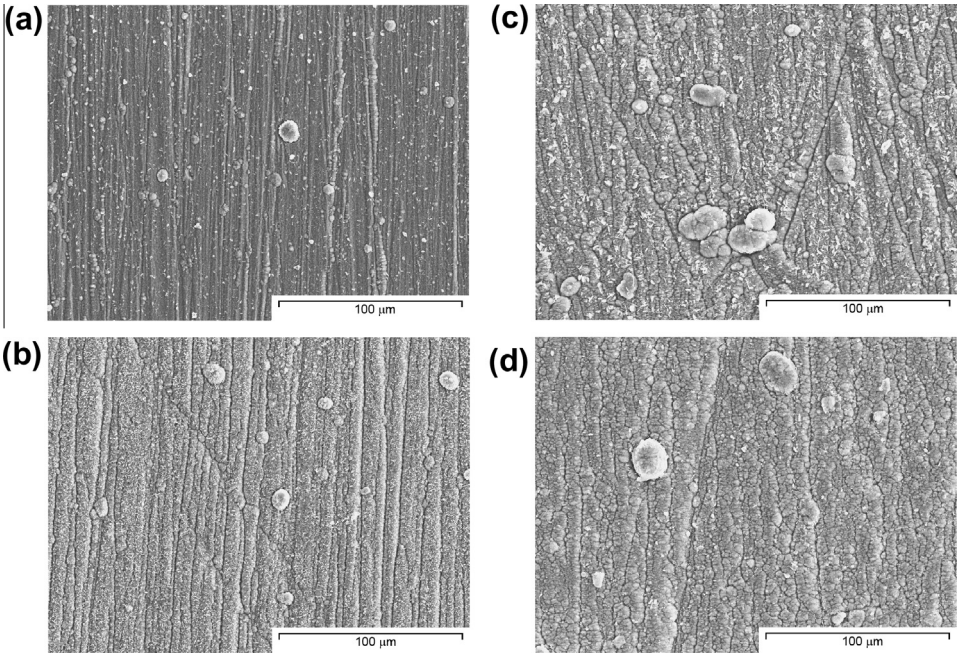

Fig. 4. Scanning electron microscopy of the surfaces of oxidised (a) CrAlN-1, (b) CrAlN-2, (c) CrAlYN-1, and (d) CrAlYN-2 coatings at 650 °C to 2000 h in 100% steam atmosphere.

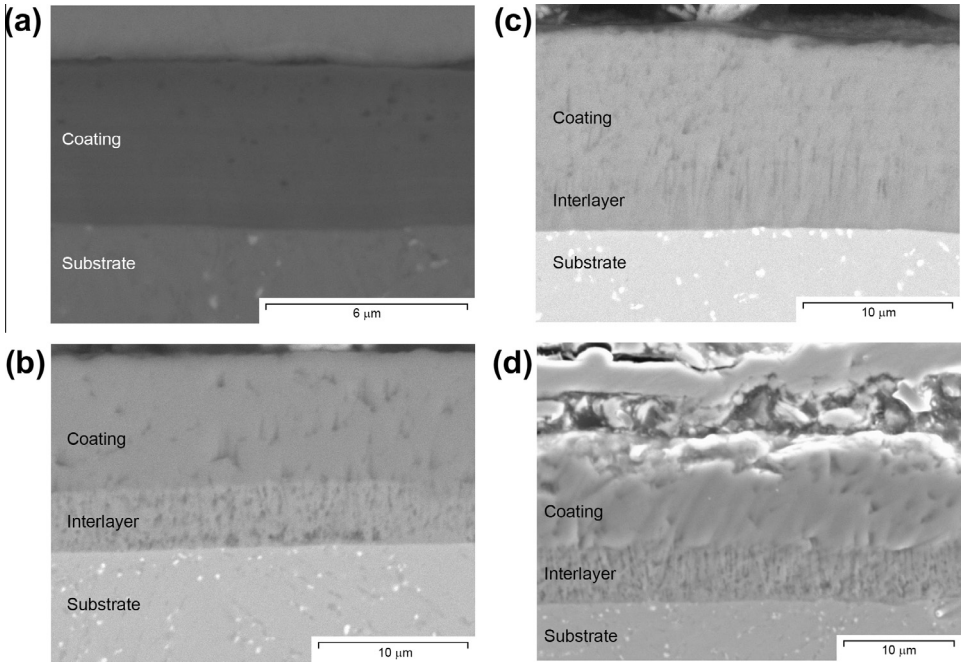

Fig. 5. Backscattered scanning electron microscopy of the cross sections of oxidised (a) CrAlN-1, (b) CrAlN-2, (c) CrAlYN-1, and (d) CrAlYN-2 coatings at 650 °C to 2000 h in 100% steam atmosphere.

bottom that is a well-known phenomenon in GDOES [17]. Also of interest, the composition profile of the CrAlN-2 specimen evidences the de-nitridation of the bulk coating. In contrast, in the depth profiles of the CrAlN-1 specimen the nitrogen signal is constant throughout the coating thickness, except for the superficial decrease due to oxide formation. In this coating only, the chromium signal indicates the development of a chromium-rich oxide near to the surface coating.

4. Discussion

In this study the oxidation behaviour of four CrAlN based coatings have been explored in 100% steam atmosphere at 650 °C. Numerous studies on the oxidation resistance of CrAlN coatings have shown their good performance in air by the development of a protective oxide scale of a mixture of Cr_2O_3 and Al_2O_3. Likewise, their thermal stability and corrosion resistance in air can be improved by additions of reactive elements such as Y, which segregate to the oxide scale grain boundaries impeding oxygen migration [13]. However, extrapolation of these results cannot be granted when oxidation is taking place in a steam atmosphere, since in many systems the conjunction of a high temperature water vapour and oxides have been reported to lead to the formation of volatile hydroxides [18].

A comparison between the data obtained for the P92 substrate and the coatings observed in Fig. 3 reveals that any of the substrate-coating systems tested represents a significant improvement of the corrosion resistance of the bare substrate. Nevertheless, the CrAlN-1 coating shows the best oxidation resistance according to its negligible mass change. The coatings studied in the present work exhibit comparable oxide growth rates to diffusion aluminide coatings that pursued a similar objective of improving the performance of P92 in steam turbines [19,20].

The SEM micrographs, GDOES and EPMA analysis corroborate the idea of the presence of aluminium/chromium protective superficial oxide layers that prevent further ionic diffusion in the four coatings. However, the CrAlN-1 coating GDOES spectrum reveals the development of a marked chromium-rich oxide layer of higher protective ability regarding the optimum coating performance. Besides the superficial oxide layers, an inner oxidation of the chromium nitride interlayer occurs at the coating/substrate interface of those coatings with adhesion interlayer. It can be assumed that the weight gain is mainly due to the adsorption of oxygen by the coating during oxidation and the development of oxidised phases. Then, the higher mass gains measured after the steam tests of the CrAlN-2, CrAlYN-1 and CrAlYN-2 coatings compared to that of the CrAlN-1 coating is related to the oxidation of the CrN adhesion interlayer. The resultant oxide inner layer suggests there is an inward diffusion of oxygen ions from the atmosphere through the coating, indicating a lower protection provided by these coatings compared to that of the CrAlN-1 coating. However, this inner oxynitride layer prevents interdiffusion between the coating and the substrate. On the one hand, the formation of iron oxides at the coating/substrate interface and the inward diffusion of oxygen in the steel substrate are undetected. On the other hand, regarding the GDOES spectra at 700 h of oxidation, the outward diffusion of iron ions from the substrate through the coatings is comparable for all four coatings. The behaviour of the chromium oxynitride layer should be tested at higher temperatures to clarify its role as a possible diffusion barrier. Additionally to nitride [7,21,22] and oxide [23] layers, also oxynitride layers have been reported to act as effective diffusion barriers [24].

Consequently, the protectiveness of the superficial oxide developed on the coatings appears to be compromised by the structure of the coating on which the oxide layers grow. Hence, tailoring the composition of coatings with the ability to develop protective films on the surface in extreme environmental conditions is not sufficient to assure a good performance of the coating but other factors should be taken into account.

The main difference between CrAlN-1 and the CrAlN-2 systems is the presence of a CrN adhesion interlayer. The deposition of a thin layer of CrN is a widely used method to improve the bond of transition metal nitride coatings deposited by PVD to the substrates, in particular for soft steel [25,26]. Furthermore, Sanchez–Lopez et al. observed a change of coating morphology when

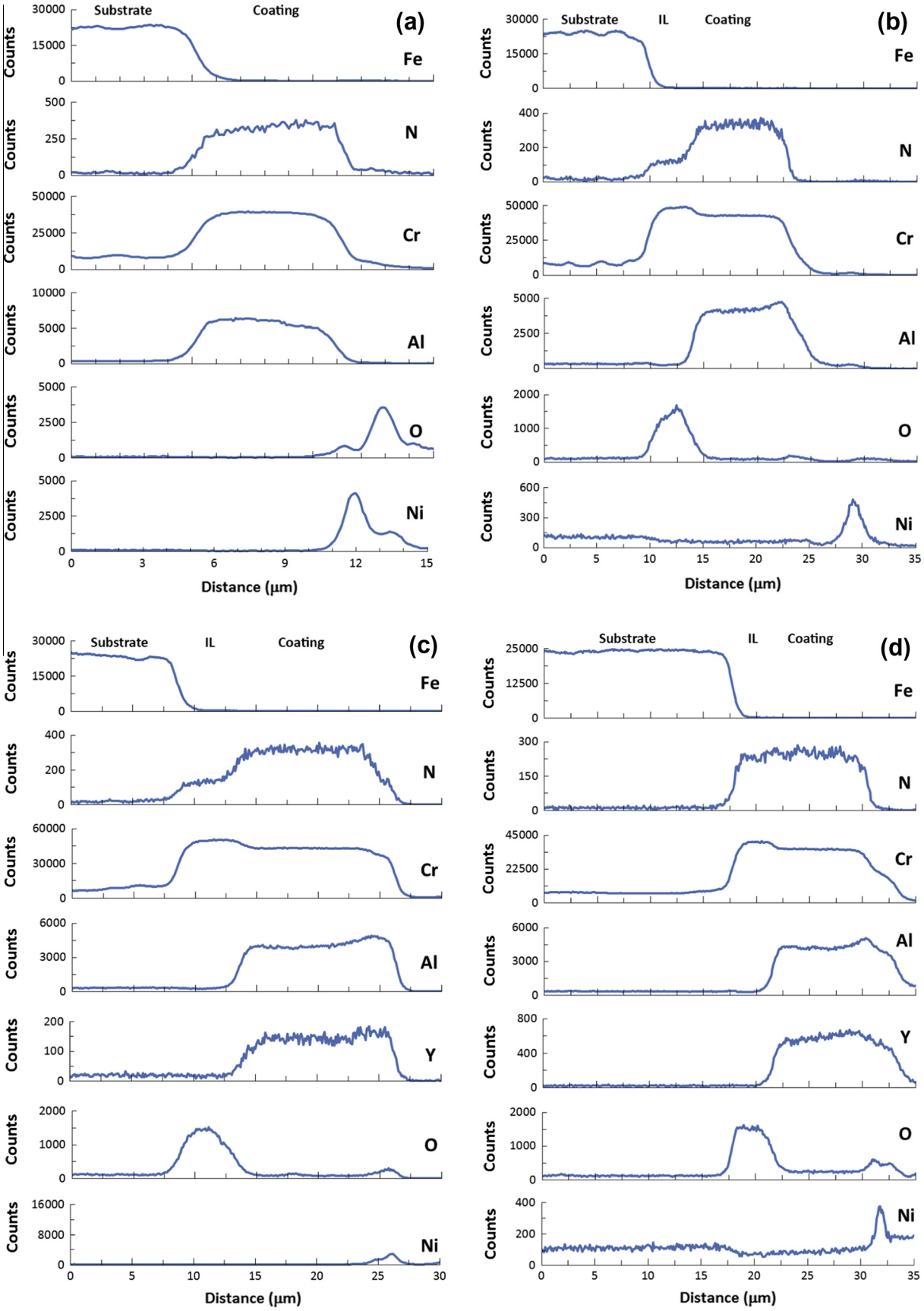

Fig. 6. Compositional depth profiles by EPMA of oxidised (a) CrAlN-1, (b) CrAlN-2, (c) CrAlYN-1, and (d) CrAlYN-2 coatings at 650 °C to 2000 h in 100% steam atmosphere. The IL acronym stands for the CrN adhesion interlayer.

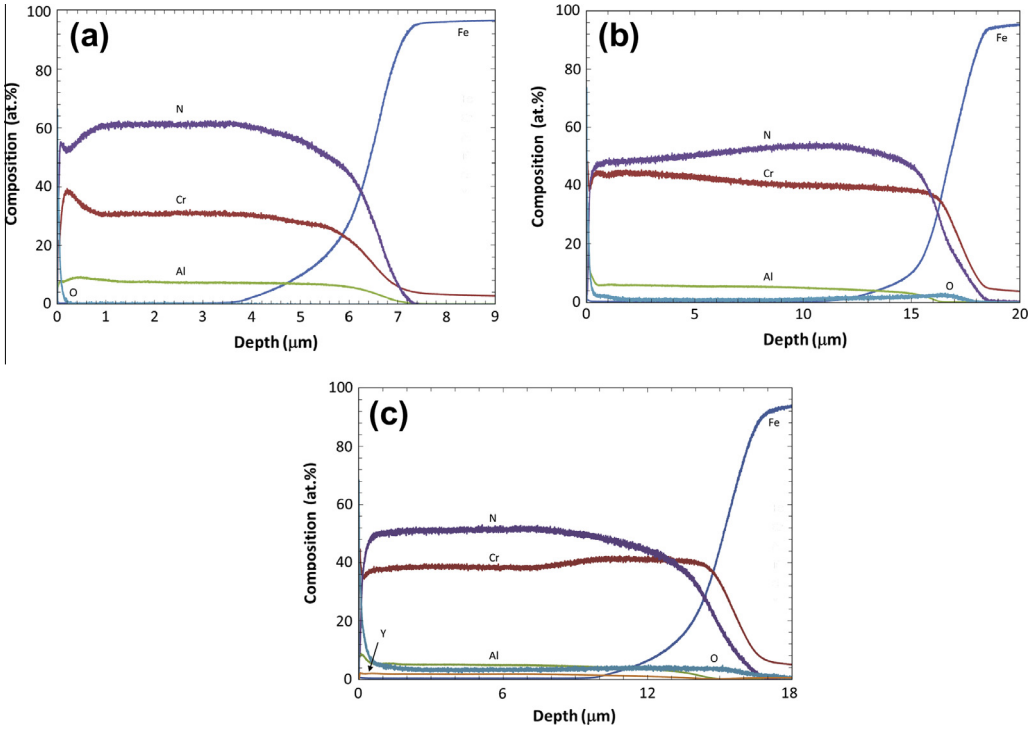

Fig. 7. Compositional depth profiles obtained by GDOES of oxidised (a) CrAlN-1, (b) CrAlN-2, and (c) CrAlYN-1 coatings at 650 °C to 700 h in 100% steam atmosphere.

including aluminium in magnetron-sputtered CrN coatings from being highly columnar to a denser microstructure [27]. This characteristic feature has a clear influence on the microstructure developed by the subsequent coating. Therefore, it is reasonable to expect a template effect of the CrN adhesion layer promoting the growth of coatings (CrAlN-2, CrAlYN-1 and CrAlYN-2) with a dissimilar grade of compactness compared to that deposited on the bare steel (CrAlN-1).

The oxygen migration is facilitated along the columnar grain boundaries through the less dense nitride coating deposited on the CrN adhesion layer. Thus, the multilayered systems formed by CrAl(Y)N coating/CrN adhesion layer/substrate result in a less protective ability than the CrAlN coating/substrate system. Of interest here is the work carried out by Franz et al., who observed an oxidised coating layer near the substrate in AlCrVN coatings after annealing at 700 °C. They associated this to the oxygen diffusion during the oxidation process along the boundaries of characteristic columnar grains of arc-evaporated coatings [28]. Additionally, the de-nitridation process, which occurred during oxidization of the coatings with the adhesion layer due to nitrogen ions migrating through the coating to the surface, seems to be facilitated. This assumption is supported by the oxidation kinetics after 1000 h of exposure and taking into account that no delamination of the coating was observed by either visual examination or SEM observations of the cross sections of oxidised coatings. The reduction of nitrogen content has been reported previously by several authors for the oxidation of PVD CrAlN based coatings but in air and above 700 °C [5,7,29]. De-nitridation by the release of N_2 was associated with the formation of oxide phases when long-term oxidation at high temperature was carried out on other nitride coating systems [30,31].

Regarding the possible additional benefits in the oxidation resistance by incorporating small concentrations of yttrium into the CrAlN coatings (0.4 at.% and 1.7 at.%), no clear conclusion can be obtained. Some mechanisms proposed in the literature explain that yttrium presence retards diffusional processes when thermal treatment is carried out in air, including selective segregation to scale grain boundaries and to the coating/scale interface [10]. Although a similar effect could be expected to that observed in air oxidation, a different mechanism is anticipated in steam oxidation regarding the oxidation kinetics of the studied coatings. The oxidation data showed in Fig. 3 reveal a higher mass gain of the CrAlYN-based coatings and shorter times for the complete oxidation of the CrN interlayer than those of the CrAlN-2 coating. This result implies that yttrium addition cannot compensate for the open grain boundaries present in the structure or this last factor is of primary importance. Additionally, the weight decrease after 1000 h of oxidation of the CrAlYN-1 and CrAlYN-2 coatings suggests that the de-nitridation process is also affected by the yttrium presence in the coatings indicative of a lower stability. Nevertheless, further studies on highly dense coatings are needed to elucidate the influence of yttrium in the steam oxidation mechanism.

Undeniably, thickness is an important parameter to fix in a coating system design. Deposition of thick coatings is ideal to act as diffusion barriers to prevent high temperature oxidation of the substrate but involves higher costs and longer production times. The results of this study demonstrate that layer thickness can be decreased without deterioration of corrosion protection by optimising of the film properties (structure and composition). Thus, the best protection is achieved with the CrAlN-1 coating whose thickness is approximately half of that of the second best performing coating (CrAlN-2).

5. Conclusions

The protectiveness of CrAl(Y)N coatings deposited by reactive magnetron sputtering on P92 steel against steam oxidation at 650 °C have been explored. During oxidation, all the coatings develop a superficial mixed chromium and aluminium oxide layer that prevents the CrAl(Y)N-based coatings from further corrosion. However, this protective oxide layer cannot avoid the oxidation of the CrN adhesion interlayer when it is present in the coating. This is explained by the lower oxidation resistance of the CrN

and the oxygen migration through more open film structures developed on top of it. However, the formation of this oxynitride barrier at the coating/substrate interface avoids the diffusion and subsequent oxidation of metals present in the steel. The possible beneficial effect of yttrium in the coating composition, regarding previous findings in similar coatings oxidised in air, is not evidenced. The yttrium role could be hidden by the effect of the grain structure that facilitates the inward oxygen diffusion. As a final remark, a CrAlN dense coating of around 6 μm without adhesion interlayer is sufficient to prevent the oxidation of the bare P92 substrate.

Acknowledgements

The authors gratefully acknowledge the financial support of the Spanish *MINECO* (projects Consolider FUNCOAT CSD2008-00023 and NANOPROTEXT MAT2011-29074-C02-01/02). Dr. R. Escobar Galindo acknowledges financial support through Ramon y Cajal Spanish programme (RyC2007-0026). Dr. S. Mato acknowledges Mr. and Mrs. Bartlett for their review of the final manuscript.

References

[1] S. Ulrich, H. Holleck, J. Ye, H. Leiste, R. Loos, M. Stüber, P. Pesch, S. Sattel, Influence of low energy ion implantation on mechanical properties of magnetron sputtered metastable (Cr, Al)N thin films, Thin Solid Films 437 (2003) 164–169.
[2] A.E. Reiter, V.H. Derflinger, B. Hanselmann, T. Bachmann, B. Sartory, Investigation of the properties of $Al_{1-x}Cr_xN$ coatings prepared by cathodic arc evaporation, Surf. Coat. Technol. 200 (2005) 2114–2122.
[3] M. Brizuela, A. Garcia-Luis, I. Braceras, J.I. Oñate, J.C. Sanchez-Lopez, D. Martinez-Martinez, C. Lopez-Cartes, A. Fernandez, Magnetron sputtering of Cr(Al)N coatings: mechanical and tribological study, Surf. Coat. Technol. 200 (2005) 192–197.
[4] J. Vetter, E. Lugscheider, S.S. Guerreiro, (Cr:Al)N coatings deposited by the cathodic vacuum arc evaporation, Surf. Coat. Technol. 98 (1998) 1233–1239.
[5] O. Banak, P.E. Schmid, R. Sanjinés, F. Lévy, High-temperature oxidation resistance of $Cr_{1-x}Al_xN$ thin films deposited by reactive magnetron sputtering, Surf. Coat. Technol. 163–164 (2003) 57–61.
[6] S. Hofmann, H.A. Jehn, Oxidation behavior of CrN_x and (Cr, Al)N_x hard coatings, Werkstoffe und Korrosion 41 (1990) 756–760.
[7] R. Escobar Galindo, J.L. Endrino, R. Martinez, J.M. Albella, Improving the oxidation resistance of Al–Cr–N coatings by tailoring chromium out-diffusion, Spectrochim. Acta Part B 65 (2010) 950–958.
[8] K.D. Bouzakis, N. Michailidis, S. Gerardis, G. Katirtzoglou, E. Lili, M. Pappa, M. Brizuela, A. Garcia-Luis, R. Cremer, Correlation of the impact resistance of variously doped CrAlN PVD coatings with their cutting performance in milling aerospace alloys, Surf. Coat. Technol. 203 (2008) 781–785.
[9] F. Rovere, P.H. Mayrhofer, Impact of yttrium on structure and mechanical properties of Cr–Al–N thin films, J. Vac. Sci. Technol. A 25 (2007). 1336-134.
[10] F. Rovere, P.H. Mayrhofer, Thermal stability and thermo-mechanical properties of magnetron sputtered Cr–Al–Y–N coatings, J. Vac. Sci. Technol. A 26 (2008) 29–35.
[11] P. Kofstad, High-Temperature Corrosion, Elsevier Applied Science, London, 1988. Chapter 11, pp. 382–385.
[12] G. Blugan, D. Wittig, J. Kuebler, Oxidation and corrosion of silicon nitride ceramics with different sintering additives at 1200 and 1500 °C in air, water vapour, SO_2 and HCl environments – A comparative study, Corros. Sci. 51 (2009) 547–555.
[13] T.C. Rojas, S. El Mrabet, S. Domínguez-Meister, M. Brizuela, A. García-Luis, J.C. Sánchez-López, Chemical and microstructural characterization of (Y or Zr)-doped Cr–Al–N coatings, Surf. Coat. Technol. 211 (2012) 104–110.
[14] J. Leal, G. Alcalá, F.J. Bolívar, L. Sánchez, M.P. Hierro, F.J. Pérez, Simulation and experimental approach to CVD-FBR aluminide coatings on ferritic steels under steam oxidation, Corros. Sci. 50 (2008) 1833–1840.
[15] E. Kotai, Computer methods for analysis and simulation of RBS and ERDA spectra, Nucl. Instrum. Methods Phys. Res. B 85 (1994) 588–596.
[16] R. Escobar Galindo, E. Fornié, J.M. Albella, Interfacial effects during the analysis of multilayer metal coatings by radio-frequency glow discharge optical emission spectroscopy. Part 1. Crater shape and sputtering rate effects, J. Anal. At. Spectrom. 20 (2005) 1108–1115.
[17] K. Shimizu, H. Habazaki, P. Skeldon, G.E. Thompson, G.C. Wood, Non-uniform sputtering and degradation of depth resolution during GDOES depth profiling analysis of thin anodic alumina films grown over rough substrates, Surf. Interface Anal. 27 (1999) 950–954.
[18] E.J. Opila, N.S. Jacobson, D.L. Myers, E.H. Copland, Predicting oxide stability in high-temperature water vapour, JOM 58 (2006) 22–28.
[19] L. Sánchez, F.J. Bolívar, M.P. Hierro, F.J. Pérez, Temperature dependence of the oxide growth on aluminized 9–12%Cr ferritic–martensitic steels exposed to water vapour oxidation, Thin Solid Films 517 (2009) 3292–3298.
[20] A. Aguero, R. Muelas, A. Pastor, S. Osgerby, Long exposure steam oxidation testing and mechanical properties of slurry aluminide coatings for steam turbine components, Surf. Coat. Technol. 200 (2005) 1219–1224.
[21] L. Zhu, S. Zhu, F. Wang, Preparation and oxidation behaviour of nanocrystalline Ni+CrAlYSiN composite coating with AlN diffusion barrier on Ni-based superalloy K417, Corros. Sci. 60 (2012) 265–274.
[22] F. Khatkhatay, J. Jian, L. Jiao, Q. Su, J. Gan, J.I. Cole, H. Wang, Diffusion barrier properties of nitride-based coatings on fuel cladding, J. Alloys Compd. 580 (2013) 442–448.
[23] W.Z. Lia, Y.Q. Lia, Q.M. Wangb, C. Sunb, X. Jiang, Oxidation of a NiCrAlYSi overlayer with or without a diffusion barrier deposited by one-step arc ion plating, Corros. Sci. 52 (2010) 1753–1761.
[24] H.C. Kim, T.L. Alford, Investigation on diffusion barrier properties of reactive sputter deposited $TiAl_xN_yO_z$ thin films for Cu metallization, Thin Solid Films 449 (2004) 6–11.
[25] X.Z. Ding, X.T. Zeng, Y.C. Liu, J. Wei, P. Holiday, Influence of substrate hardness on the properties of PVD hard coatings, Synth. React. Inorg., Met.-Org., Nano-Metal Chem. 38 (2008) 156–161.
[26] P. Yashar, S.A. Barnett, J. Rechner, W.D. Sproul, Structure and mechanical properties of polycrystalline CrN/TiN superlattices, J. Vac. Sci. Technol. A 16 (1998) 2913–2918.
[27] J.C. Sánchez-López, D. Martínez-Martínez, C. López-Cartes, A. Fernández, M. Brizuela, A. García-Luis, J.I. Oñate, Mechanical behavior and oxidation resistance of Cr(Al)N coatings, J. Vac. Sci. Technol. A 23 (2005) 681–686.
[28] R. Franz, J. Schnöller, H. Hunter, C. Mitterer, Oxidation and diffusion study on AlCrVN hard coatings using oxygen isotopes ^{16}O and ^{18}O, Thin Solid Films 519 (2011) 3974–3981.
[29] J. Lin, B. Mishra, J.J. Moore, W.D. Sproul, High temperature oxidation behavior of CrN/AlN superlattice films, Surf. Coat. Technol. 202 (2008) 3272–3283.
[30] S. Danaher, T. Dudziak, P.K. Datta, R. Hasan, P.S. Leung, Long-term oxidation of newly developed HIPIMS and PVD coatings with neuronal network prediction modelling, Corros. Sci. 69 (2013) 322–337.
[31] K. Katuku, A. Koursaris, I. Sigalas, High-temperature stability of polycrystalline cubic boron nitride cutting tool materials in air, Corros. Sci. 64 (2012) 55–63.